Proceedings of Ninth World Conference on Earthquake Engineering
August 2-9, 1988, Tokyo-Kyoto, JAPAN (Vol.IV)

6-4-4

THEORETICAL ANALYSIS ON DEFORMATION CAPACITY OF R/C MEMBERS

Hisahiro HIRAISHI[1], Eiichi INAI[2], and Masaomi TESHIGAWARA[1]

[1]Building Research Institute, Ministry of Construction,
[2]Tsukuba-shi, Ibaraki, Japan
[2]Technical Research Institute, Hazama-Gumi Ltd.,
Yono-shi, Saitama, Japan

SUMMARY

A lot of studies on the ductility of reinforced concrete columns have been performed by many researchers. Most of their attempts were the statistical studies based on test results, and some of the researchers investigated it theoretically by assuming a certain limit of either compressive or tension strain at the critical section. In this paper, the deformation capacity, in case of columns which fail due to the crush of concrete after flexural yielding, is defined from the point of view of energy absorption of columns. And then the equations which give the strains in the critical section at the deformation capacity are induced by the flexural theory. Finally, an equation which gives the drift angle of columns at their deformation capacity is derived from a simplified truss model.

INTRODUCTION

The deformation capacity is one of most important factors to evaluate seismic performance of structural members. However, a reasonable definition of it has not been proposed yet. The deformation at the deterioration in strength of 80% of the ultimate load is often taken as the deformation capacity of the test results, but the reason for it is not clear. Also, some researchers discussed a critical strain in the extreme compressive concrete fiber or a critical curvature at the critical section. A few researches showed that there was a critical tension strain in steel bars at the critical section (Ref. 1 and Ref. 2), and then presented the strain and curvature in the critical section at that moment. However their meaning on the deformation capacity of members was not explained well because of the difficulty in estimation of the drift of members from the strain and curvature at the critical section. This paper, based on the test results of columns (Ref. 3), shows that there is a critical point in the vertical displacement at tension side in hinge region, and that the mechanism of energy absorption in a whole column changed dramatically at the critical point, referred to as "stable limit". The drift angle of columns at this stable limit is calculated based on the strains and curvature in the critical section, and a simplified truss model which represents the deformation mechanism after flexural yielding of tension steel bars.

ENERGY ABSORPTION IN MEMBERS AND STRAINS IN A CRITICAL SECTION AT THE STABLE LIMIT

Energy Absorption in Members The amount of extension of tensile longitudinal reinforcing bars in the hinge region obtained from the tests of columns(Ref.3)

are shown in Fig. 1. There is a strong correlation between the drift angle and the amount of the extension. Figure 2 shows the amount of work done by external forces and the strain energy absorbed in longitudinal tensile steel bars and the others. The each amount of energy absorbed increase as long as the tensile bars are elongating. However, after the limit of extension of tensile bars, the mechanism of energy absorption in the columns undergoes a change as follows:

1) The amount of strain energy in tensile bars starts decreasing.
2) The amount of work done by the axial load starts increasing rapidly because of the shortening of the columns in the axial direction.
3) The amount of strain energy absorbed in the whole column, especially that in concrete starts increasing rapidly.
4) Consequently, the lateral load carrying capacity significantly starts decreasing (see Fig. 3).

From the facts mentioned above, the limit of the extension of the tensile bars in columns is considered to be the critical point for deformation capacity. This limit is hereafter referred to as "stable limit" in this paper.

Strains in a Critical Section at the Stable Limit Figure 4 shows that the strain of tensile bars in the critical section reaches the maximum at the stable limit. Assuming that the plane section before bending remains plane after bending, the value of the maximum strain in the tensile bars is obtained from the following two conditions, in case of the section shown in Fig. 5 under a constant axial load.

1) Equilibrium requirement of forces in the axial direction
2) $\frac{d\varepsilon_0}{d\varepsilon_c} = 0$ (1)

where, ε_0 = strain in tensile bar, and
ε_c = concrete strain in the extreme compressive fiber.

The solution under the assumption of the perfect elasto-plastic relation for steel is derived as follows (see Fig. 6). The detail of the solution is shown in Ref. 1 and 2, and the solution taking account of strain hardening in both tension and compression bars is shown in Ref. 3.

The maximum strain in tensile bars at the stable limit

$$\varepsilon_{0,MAX} = \underline{(S_3-S_1)/(S_1+S_2)} \cdot \varepsilon_{c,CR} \quad (2)$$

The curvature at the stable limit $\Phi_{SL} = \underline{(S_2+S_3)/(S_1+S_2)} \cdot \varepsilon_{c,CR} / (d_1 \cdot D)$ (3)

The depth of neutral axis at the stable limit $x_{n1} = \underline{(S_1+S_2)/(S_2+S_3)} \cdot d_1$ (4)

where, S_1, S_2, and S_3 = the areas shown in Fig. 6,
$\varepsilon_{c,CR}$ = the concrete strain in the extreme compressive fiber at the stable limit,
and d_1 = ratio of the distance from the extreme compressive fiber to tensile bars to depth of column.

If the stress-strain curve for concrete is simplified as three lines shown in Fig. 7, the each ratio of areas underlined in Eqs. (2), (3), and (4) will be expressed by merely the ratio of the axial stress (η_0), and Equations (2), (3), and (4) will be rewritten by Eqs. (5), (6), and (7).

$$\varepsilon_{0,MAX} = (1/\eta_0 - 1)/2 \cdot \varepsilon_{c,CR} \quad (5)$$

$$\Phi_{SL} = (1/\eta_0 + 1)/2 \cdot \varepsilon_{c,CR}/D \quad (6)$$

$$x_{n1} = 2/(1/\eta_0 + 1) \quad (7)$$

where, η_0 = ratio of axtial stress (N/bD) to compressive strength of confined concrete (fc").

If the value of η_0 is same regardless of fc", x_{n1} at the stable limit is independent of fc", and $\varepsilon_{0,MAX}$ and Φ_{SL} depend on only η_0. It is generally known that it is effective in ductility to design axial loads in low level and to improve decrease in strength after the maximum load on the stress-strain curve for concrete by lateral confinement, and that the greater Φ_{SL} and $\varepsilon_{0,MAX}$ are, the better the deformation capacity is, and also the smaller x_{n1} is, the better it is. Equations (5) ~ (7) and Figs. 6 and 7 clearly explain the effects of η_0 and the stress-strain curve for concrete on ductility.

A TRUSS MODEL REPRESENTING DEFORMATION MECHANISM

Deformation Mechanism After Flexural Yielding Typical crack pattern and distribution of strain on the both side ends along the height of a column which behaves in a ductile mode after flexural yielding are shown in Fig. 8. The inclined flexural shear cracks in hinge region tend to concentrate to the center of compressive zone at the base. In this paper, considering this crack patterns, a simplified truss model shown in Fig. 9, consisting of a inelastic concrete region, rigid members, and a non-prismatic member expressing the tensile bars in the hinge region (Ref. 4), is used to explain the deformation mechanism of columns. (Exactly speaking, a truss model in Fig. 10 may be more suitable for the deformation mechanism. However, the model shown in Fig. 9 is applicable enough for it in the large deformation range.) The sectional area at each height in the non-prismatic member is determined by the stress at each height of tensile bars obtained from equilibrium of forces on the inclined crack surface developing from its height. The deformation mechanism in Fig. 9 gives Eq. (8).

$$\text{Drift angle } R = v / \{ (d_1 - x_{n1}) D \} \tag{8}$$

where, v= vertical displacement at the top at tension side $v = h \int_0^1 \varepsilon_\eta \, d\eta$,
ε_η= strain at height of $(0 \leq \eta \leq 1)$ in the tensile bars $\varepsilon_\eta = f_s(\sigma_\eta)$,
h= height of column,
f_s= function which expresses the stress-strain relation for steel,
$x_{n1}D$= depth of neutral axis in the critical section,
$d_1 D$= distance from extreme compression fiber to the tensile bars, and
σ_η= stress in the tensile bar corresponding to ε_η .

The drift angle obtained by substituting v and of the test results into Eq. (8) are shown in Fig. 11 compared with that calculated by horizontal displacements.

Calculating of Drift Angle at Stable Limit To obtain the stress in a tensile bar, the equilibrium of forces is simplified as Fig. 12, on the assumptions that very little shear can be transferred by either interlock or dowel action and that the inclined shear cracks concentrate to the center of the compressive zone at base. Also assuming that all of the shear reinforcement and all of the central longitudinal reinforcement, if there is any, in the radiate crack zone have been yielding or nearly yielding, Equations (9) and (10) may be obtained.

$$T_W = T_{W0} \tag{9}$$

$$Q_W = bh \cdot p_W \cdot \sigma_{wy} \cdot \eta \tag{10}$$

where, T_{W0} , T_W = the sum of forces of central longitudinal reinforcement at the base and at the inclined crack surface,
p_W = ratio of the area of shear reinforcement to the area of longitudinal cross section, and
σ_{wy} = yield strength of shear reinforcement.

Therefore, from the equilibrium requirement for the free body, Equations (11) and (12) are obtained.

$$T_\eta = T_0 - b h^2 p_W \sigma_{wy} / \{(2d_1 - x_{n1})D\} \cdot \eta^2 \tag{11}$$

$$\sigma_\eta = T_\eta / (p_t bD) = \sigma_0 - \sigma_{wy} / (2d_1 - x_{n1}) \cdot (h/D)^2 \cdot (p_W / p_t) \cdot \eta^2 \tag{12}$$

where, T_0 , T_η = the sum of forces of tensile bars at the base and at the height of η, and
p_t = ratio of the area of tensile bars to the area of longitudinal cross section.

Using the assumed stress-strain relation for steel shown in Fig. 13, the distribution of strain in the non-prismatic tensile bar is expressed as follows. (So far as the large deformation range is concerned, only plastic strain is taken

into account in this paper, as there is little effect of elastic strain on the whole deformation.)

$$\varepsilon\eta=(\sigma_0-\gamma\eta^2-\sigma_y)/E_{sh}+\varepsilon_{sh}=\varepsilon_0-\gamma/E_{sh}\cdot\eta^2 \quad (13)$$

where, ε_0 = the strain of tensile bar at the base, and

$$\gamma=\sigma_{wy}/(2d_1-x_{n1})\cdot(h/D)^2\cdot(p_w/p_t).$$

The height of the hinge region is expressed by Eq. (14) as the range in which tensile bar is yielding.

$$\eta_y=\{(\varepsilon_0-\varepsilon_{sh})\cdot E_{sh}/\gamma\}^{1/2} \quad (14)$$

Hence, the value of the extension of the tensile bar in the hinge region (corresponding to v) is given by Eq. (15) on the assumption of $\sigma_{wy}=\sigma_y=E_s\cdot\varepsilon_y$.

$$v=h\int_0^{\eta_y}\varepsilon\eta\,d\eta$$
$$=D/3\,(2\varepsilon_0+\varepsilon_{sh})\cdot\{E_{sh}/E_s\cdot(\varepsilon_0-\varepsilon_{sh})/\varepsilon_y\cdot(p_t/p_w)\cdot(2d_1-x_{n1})\}^{1/2} \quad (15)$$

Also, the drift angle is expressed by the following Eq. (16).

$$R=1/3\,(2\varepsilon_0+\varepsilon_{sh})\cdot\{E_{sh}/E_s\cdot(\varepsilon_0-\varepsilon_{sh})/\varepsilon_y\cdot(p_t/p_w)\cdot(2d_1-x_{n1})/(d_1-x_{n1})^2\}^{1/2} \quad (16)$$

The drift angle at the stable limit is given by substituting the value of $\varepsilon_{0,MAX}$ (see Eq. (2)) and x_{n1} (see Eq. (4)) into Eq. (16).

The strain distribution of the tensile bar along the height obtained from the analysis is shown in Fig. 14 in comparison with the test results at the stable limit. In Fig. 14, the assumed stress-strain relation for steel in the above analysis is based on the stresses given by the reversed stress behavior, using the strain measured in tests, and is shown in Fig. 15. The test results are in excellent agreement with the analytical results.

CONCLUSIONS

The following findings were drawn from this study.

1) In the process of deformation from yielding to failure, there is a stable limit from the point of view of energy absorption of columns, even though columns are designed to behave in ductile manner. This stable limit corresponds to the limit of the extension of tensile longitudinal reinforcing bars. While the tensile bars is extending, the columns behaves on the stable load-deformation curves. After the drift angle exceed the stable limit, the lateral load carrying capacity drasticly decrease.
2) The relationships among the strain in tensile bars, the strain of the extreme compressive concrete fiber, the curvature, the depth of neutral axis in the critical section at the stable limit, the stress-strain relation for concrete and steel, and axial stress level are shown in Fig. 6, and Eqs. (2) ~ (4).
3) It is very important for estimating the deformation capacity of columns to model the stress-strain relation for confined concrete.
4) The deformation mechanism of columns after flexural yielding can be represented by the truss model proposed in this paper. The tension strain distribution along the height in the hinge region obtained from tests are in excellent agreement with the analytical value. The drift angle at the stable limit can be calculated by Eq. (16), however for practical application, a number of tests should be performed to examine its adequacy.

ACKNOWLEDGMENTS

The authors are thankful to assistant researcher T. Kawashima at Building Research Institute for his excellent help in the data analysis.

REFERENCES

1. Suzuki,K., Nakatsuka,T., and Inoue,K., "Ultimate Limit Index Points and their Characteristics of Patially Prestressed Concrete Beam Sections", Colloquium on Ductility of Concrete Structures and its Evaluation, JCI, March 28,29,1988
2. Koyanagi,W., Rokugo, K., and Iwase,h., "Toughness Evaluation and Toughness Design of Reinforced Concrete Beams", Colloquium on Ductility of Concrete Structures and its Evaluation, JCI, March 28,29,1988
3. Hiraishi,H., Inai,E., and Teshigawara,M., "Flexural Deformation Capacity of R/C Members Based on Deformation Mechanism", Colloquium on Ductility of Concrete Structures and its Evaluation, JCI, March 28,29,1988
4. Hiraishi,H., "Analytical Study on Load vs. Deformation Relationship of Flexural Type Reinforced Concrete Shear Wall", Journal of Structural and Construction Engineering, 1985, January

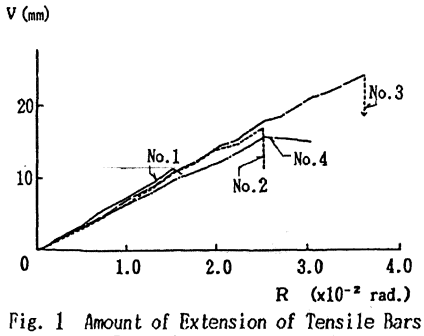

Fig. 1 Amount of Extension of Tensile Bars Drift Angle

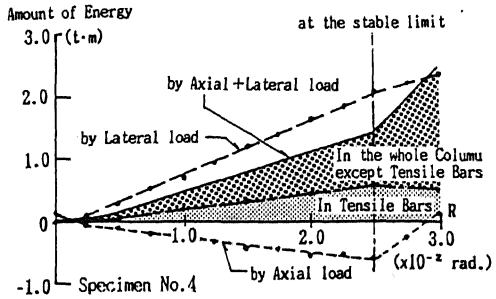

Fig. 2 Amount of Work done by External Forces and Each Amount of Strain Energy

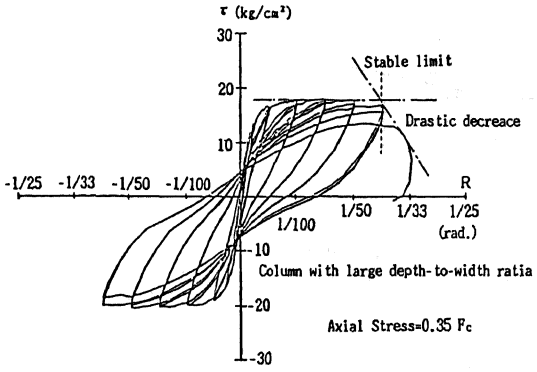

Fig. 3 τ (Average Sear Stress) R (Drift Angle)

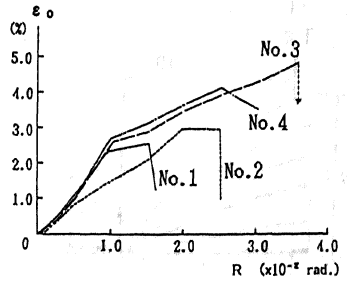

Fig. 4 Tension Strain in Bars at the Criotical Section Drift Angle

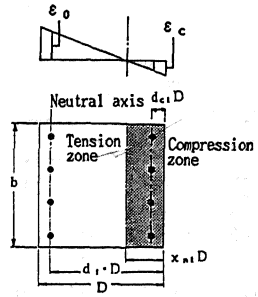

Fig. 5 A Symmetrical Section

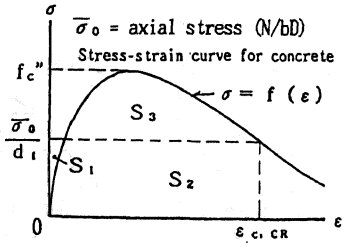

Fig. 6 Assumed Stress-Strain Relation for Concrete and Axial Stress

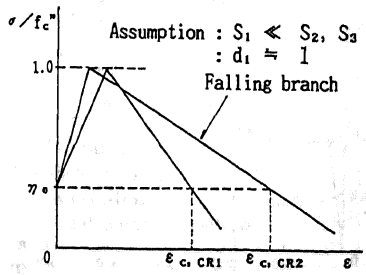

Fig. 7 Idealized and Normalized by fc" Stress-Strain Relation for Concrete

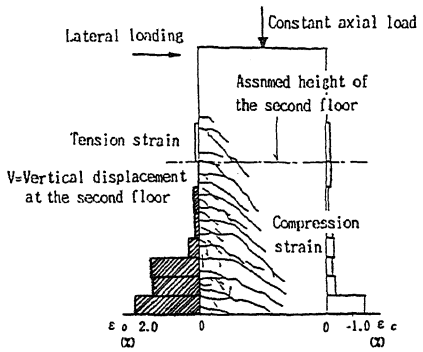

(Specimen No.1 the drift angle =1/100 rad.)

Fig. 8 Crack Pattern and Strain Distribution Along the Height at Both Side Ends

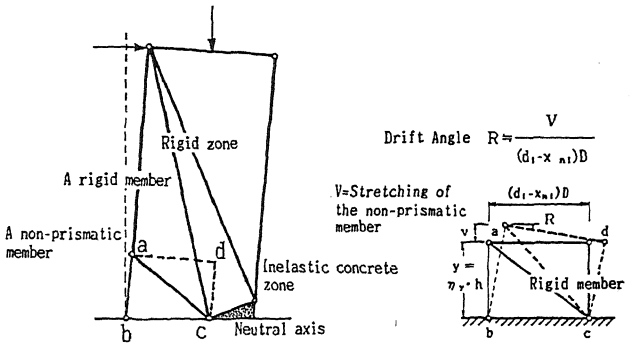

Fig. 9 A Simplified Truss Model and Deformation Mechanism

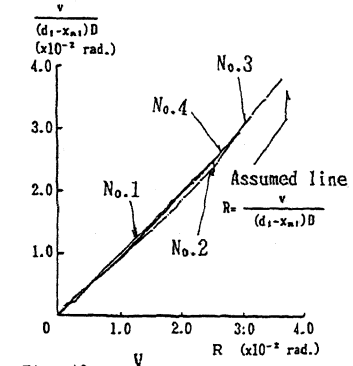

Fig. 10 $\frac{V}{(d_1-X_{n1})D}$ versus R

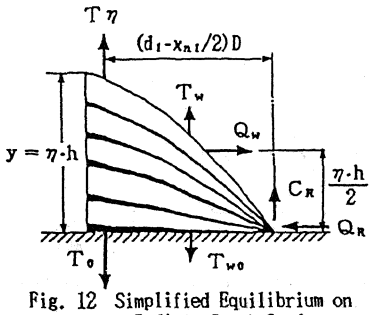

Fig. 12 Simplified Equilibrium on a Radiate Crack Surface

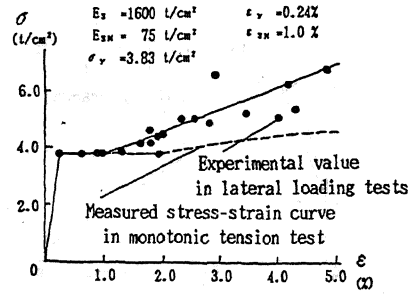

Fig. 15 Used Stress-Strain Relation for Steel in the Analysis

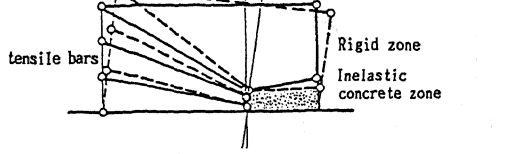

Fig. 11 A Truss Model Representing the Deformation Mechanism in the Radiate Crack Zone

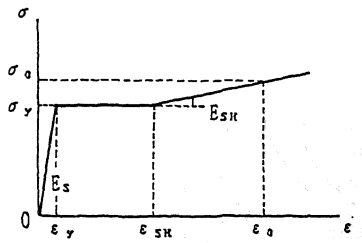

Fig. 13 Assumed Stress-Strain Relation for Longitudinal Steel Bar

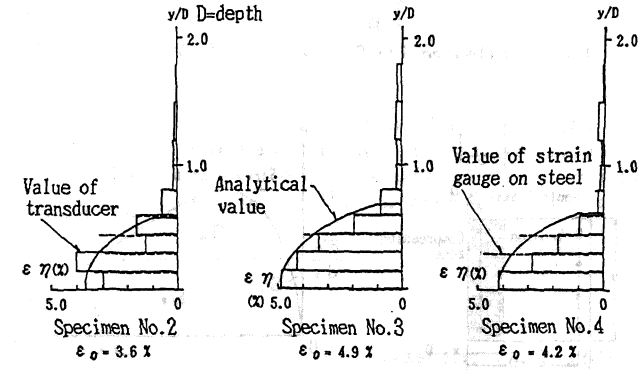

Fig. 14 Comparisons of Analytical Strain Distribution in Tensile Bar Along the Height with Test Results